Theoret. chim. Acta (Berl.) 28, 151—160 (1973)

Photodecomposition of Ketene to Form Methylene

Harold Basch

Department of Chemistry, Bar Ilan University, Ramat Gan, Israel

Received September 13, 1972

Correlation curves for a least motion departure path of methylene in the photocomposition of ketene are interpreted in terms of least energy paths. It is concluded that the first excited triplet state of ketene can probably form $^3CH_2(^3B_2)$ and $^1CH_2(^1A_1)$ relatively rapidly and the first excited singlet state can give $^3CH_2(^3B_2)$ easily in a near least motion path. However, the formation of $^1CH_2(^1A_1)$ from the first excited singlet state of ketene by a near-least motion path appears to be highly improbable.

Die Korrelationskurven des Reaktionswegs mit dem geringsten anfänglichen Bewegungsaufwand des Methylens, das durch Photozersetzung des Ketens gebildet wird, werden mit Hilfe des Reaktionswegs geringster Energie interpretiert. Es wird gefolgert, daß sich aus dem ersten angeregten Triplettzustand des Ketens wahrscheinlich relativ schnell $^3CH_2(^3B_2)$ und $^1CH_2(^1A_1)$ bilden können und daß die Bildung von $^3CH_2(^3B_1)$ aus dem ersten angeregten Singulettzustand auf einem Weg, der näherungsweise dem eingangs genannten entspricht, erfolgt. Die Bildung von $^1CH_2(^1A_1)$ nach diesem Reaktionsweg ist dagegen sehr unwahrscheinlich.

Introduction

Although the chemical reactions of methylene (CH_2) in both its ground triplet ($^3CH_2$) and lowest energy singlet ($^1CH_2$) electronic[2] states are under extensive study, both experimentally and theoretically, very little is yet known about the intrinsic mechanism of the photodecomposition process by which methylene is initially generated from, for example, ketene. A knowledge of the mechanism of this reaction, as given by the potential energy surface governing the motion of the species involved, could lead to the resolution of such important but experimentally difficult questions as what are the initial kinetic and internal energies of the methylene and their primary photon energy dependencies. The lack of information about the specific vibrational level or even electronic state in which the methylene is initially formed in the photolysis experiment clearly clouds any conclusions or analysis based on subsequent methylene reactions.

Methylene is obtained in the photolysis of ketene up to the highest wavelength possible (~ 3660Å) thermodynamically consistent with the known energetics of the over-all $CH_2CO = CH_2 + CO$ reaction [1]. However, the reaction apparently requires an activation energy [2, 3]. Quantum yields for photodissociation are found to be much less than unity and variable with temperature pressure and wavelength (for $\lambda \geqq 3130$Å). These characteristics, especially the pressure dependence, indicate that the ketene excited electronic state or states populated in the photolysis process is (are) long-lived. It has also been established that at all but the highest wavelengths singlet methylene is obtained in higher yield than triplet methylene, although both are obtained above 2600Å [4]. Interestingly enough, the recombination reaction ($CO + CH_2$ to make ketene) is much faster

with $^3CH_2$ than with $^1CH_2$ [4, 5]. A complicating factor in describing the photodissociation reaction mechanism is the recent series of ^{14}C experiments [5, 6]. In the reaction of methylene containing radioactive ^{14}C with CO the product ^{14}CO is found with $^1CH_2$ but not with $^3CH_2$ as the initial methylene reactant. Conversly, the photolysis of selectively labelled ketene ($^{14}CH_2CO$) produces ^{14}CO in significant percentage yield that increases with time and decreased pressure. Any proposed mechanism for the $CH_2CO = CH_2 + CO$ system should be consistent with the known properties of the process as well, of course, as with the ultraviolet spectroscopy of ketene itself.

The electronic spectrum of ketene has been reported and discussed several times with very little agreement about its assignment [7–9]. According to Laufer and Keller [9] the gas phase absorption spectrum in the 4700–2600Å range consists of diffuse bands superimposed on a broad continuum and peaking at about 3.75 eV; the total system representing a single electronic transition. This last conclusion differs with all previous opinions on the number of distinct electronic states appearing in this wavelength region. The diffuseness presumably arises from predissociation of the vibronic levels leading to the dissociation into CH_2 and CO fragments. The transition is characteristically weak [7] and with intensity similar to the electric dipole forbidden $^1A_2(n, \pi^*)$ transition in formaldehyde. The vibrational mode of the band progressions has been identified as the in-plane bending mode of the skeletal C–C–O fragment. Thus presumably in its equilibrium geometry this state is strongly in-plane bent. The next absorption systems begins at about 2130Å and consists of a series of 4 sharp bands of decreasing intensity with an average energy separation of about 1040 cm^{-1} [8].

An assignment of the long wavelength transition as well as identification of the electronic states important in the photolysis process requires an enumeration and description of the molecular orbitals (MO *s*) of ketene and their correlation with the combined orbital description of CH_2 and CO. In C_{2v} symmetry with the molecule in the *xz* plane the ground electronic structure of ketene in primarily $\ldots 7a_1^2\, 2b_1^2\, 2b_2^2$ (b_2 transforms as the coordinate *y*) where the convention of listing only the highest occupied MO of a given representation has been adopted. The simplest possible path for the photodissociation process is for CH_2 and CO to separate along the linear C–C=O axis, preserving C_{2v} symmetry at all separations. We call this path the least motion departure (or approach) path and any deviation from this path obtained by a modest angular (in plane or out of plane) motion of the CO relative to planar CH_2 (including radial displacement of the fragments and reorientation of the carbonyl, for example) a near-least motion path.

Qualitative Considerations

For the least motion path it is possible to draw the schematic correlation diagram shown in Table 1. Here the familiar low-lying electronic states of methylene [10–12] combined with the ground state electronic configuration of CO($^1\Sigma^+$) on the right hand side are connected to the corresponding electronic states of normal ketene on the left side. The energy ordering of the ketene states is obtained by the usual considerations; ground ($^1A_1$) state lowest, singly excited triplet ($^3B_2$)

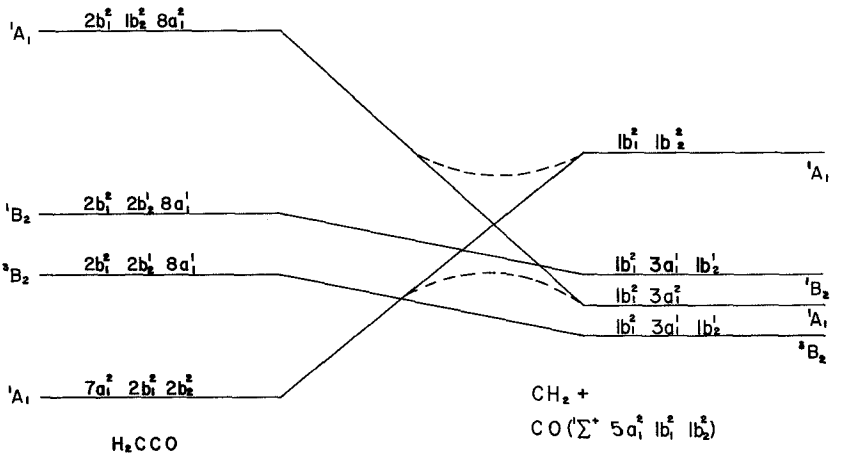

Fig. 1. Schematic state correlation diagram for the least motion path in $H_2CCO = CH_2 + CO$

state next, corresponding singlet ($^1B_2$) next, and doubly excited singlet ($^1A_1$) state highest in energy. Although the energy ordering of the methylene states are well established, the total energy spread between the $^3B_2$ and upper $^1A_1$ states is not known precisely but certainly does not exceed 4eV [10, 11]. The $^1CH_2$ state referred to previously is to be identified with the lower $^1A_1$ CH_2 state and $^3CH_2$ with the $^3B_2$ state of Fig. 1.

The simple correlation diagram in Fig. 1, although strictly relevant only to the least motion path and is, as we will see, incomplete since it omits certain very relevant states, is informative. The non-identification of the ground ($^1A_1$) state electronic configuration of ketene with the combined fragments lowest energy $^1A_1$ state electronic configuration leads to an avoided crossing of these curves at intermediate separations due to configuration interaction (dashed lines). This in return predicts the presence of a barrier to chemical reaction in forming ketene from $CH_2(^1A_1)$ and $CO(^1\Sigma^+)$ by a least motion approach. In the terminology of Hoffmann and Woodward [13] the path is "forbidden" and the concerted reaction will probably proceed (if at all) by some other path in which the barrier is, at least, much reduced, if not completely absent. Based on the previous work of Hoffmann and co-workers [14] a reasonable guess at the most favourable path can be made. The least energy path is expected to involve an initially perpendicular attack of CO on the methylene plane where the carbonyl carbon lone pair is approaching the empty $1b_2$ MO of the methylene carbon.

In any event the ground $^1A_1$ state of ketene does connect with the lowest energy $^1A_1$ state of combined $^1CH_2 + CO$, contrary to previous descriptions, [4, 10, 15] and $^1A_1$ is the lowest energy singlet electronic state along the least energy path. This in turn requires that the formation of $^1CH_2$ from the excited singlet electronic state of ketene, as presumably happens in the photolysis experiment, must involve the close overlap and coupling of the vibronic levels of this latter photolysis state and the ground $^1A_1$ state in a low energy region; their direct connection being precluded even in the absence of symmetry elements.

Calculations on the low-lying electronic states of ketene has consistently predicted [7, 8, 15] the lowest energy state to be of A_2 symmetry arising out of a $2b_2 \rightarrow 3b_1$ one electron transition. In Fig. 1 no states of A_2 symmetry appear. Since the b_2 and b_1 representations in C_{2v} symmetry correlate with the π_x and π_y of the carbonyl $C_{\infty v}$ local symmetry the terminating state of this transition in ketene will correlate with one of the excited states of the free CO molecule which begin at ~ 6eV above its ground state. Thus the $^{3,1}A_2$ states which presumably lie immediately above the ground state of ketene connect to combined fragment states higher in energy than in all the $CH_2 + CO(^1\Sigma^+)$ states shown in Fig. 1.

Of course, if the band system observed in the long wavelength region of the ketene spectrum is identified with the calculated A_2 state then the longest wavelength transitions are to a strongly in-plane bent geometric conformer of that state. The lower symmetry of the bent geometry will allow configuration mixing with the like-spin B_2 states of Fig. 1 (to give A'' states in C_s symmetry).

This is important since, as it appears from Fig. 1, the relative ordering of the lowest A_2 and B_2 states inverts on going from normal ketene to the dissociated $CH_2 + CO$ fragments and thus would be expected to cross in the least motion path symmetry (C_{2v}). The resultant avoided crossing in the lower symmetry (C_s) allows a direct connection between the $^3A_2$ state of normal ketene and the $^3CH_2 + CO(^1\Sigma^+)$ combined fragment ground states with a barrier for dissociation. Again, the magnitude of this barrier is departure geometry dependent and in the least energy path for this state possibly wholly absent.

Results

In order to obtain more quantitative information about the behavior of all these states as a function of $CH_2 - CO$ separation *ab initio* single and multi configuration self consistent field (SCF) calculations were carried out in an extended basis set of contracted gaussian orbitals. The geometry of the CH_2 and CO fragments were frozen at their normal ketene values [11] and calculations carried out at C – C distances (R) identified by their difference from the normal ketene value; *i.e.* $\Delta R = 0, 2, 4,$ and 10 a.u. The basis set was taken as Dunning's 4^s, 2^p contraction [17] of Huzinaga's (9^s, 5^p) C and O atom gaussian sets [18]. The carbon atom basis sets were each augmented by a single two component orbital of s-type with analytical form, 0.690445(0.01918) + 0.3296448(0.009401) to mimic a 3*s* atomic orbital. Here the exponents are in parenthesis preceded by the respective gaussian function expansion coefficient and both were chosen based on previous work [19–22]. The need for extravalent basis orbitals of this type is demonstrated for the B_2 states. For the hydrogen atom Huzinaga's 4^s set was scaled by a factor of $(1.2)^2$ and the smallest exponent member split off to form a separate basis function, as previously [21]. The final basis set is thus 36 functions contracted from 84 gaussians.

Open shell single configuration SCF calculations were carried out on the lowest energy $^{1,3}B_2$ and $^{1,3}A_2$ electronic states of ketene. The former states arise out of the $2b_2 \rightarrow 8a_1$ one electron transition from the ketene ground state electronic configuration. Since the $^{1,3}A_2$ states arising out of the $2b_2 \rightarrow 3b_1$ excitation correlate with the excited electronic states of the CO molecule at large interfrag-

ment separations the single configuration wave functions valid for these states in normal ketene are not proper space eigenfunction for the corresponding CO states due to the neglect of averaging over degenerate π_x and π_y orbital occupancies. Therefore, single configuration SCF results were obtained only at $\Delta R = 0$ and 2 a.u. for the A_2 states. This situation can be treated correctly and automatically by a configuration interaction approach of the open shell states at all R; in which case the proper degeneracies would appear naturally at large R.

The single configuration SCF computer programs used in this study have been described previously [20]. Essentially the orthogonality constrained method described by Segal [23] is used to solve the SCF equations. Careful checking revealed no initial input dependence of any SCF result reported here.

For the $^1A_1$ states of ketene at all R multi configuration SCF calculations were carried out using all 6 possible configurations arising from the distribution of 2 spin-paired sets of electrons among 4 orbitals ($7a_1$, $2b_2$, $8a_1$, and $3b_2$). Both configuration and basis orbital expansion coefficients were simultaneously optimized in the usual variational procedure [24, 25]. The Fock-type equations for the orbitals are similar to those described in detail previously and the equations were solved for in the same orthogonality constrained manner [24]. This particular set of configurations were chosen based on a consideration of Fig. 1 and a previous such study on ethylene [24]. An additionally important consideration was the expectation that in using a more restricted number of configurations the orbital nature of the $8a_1$ MO would be strongly dependent on the choice of configurations. Essentially, the problem revolves about the point that the occupancies of the $2b_2$ and $8a_1$ MO's are strong functions of R as shown in Fig. 1. It follows then that the $8a_1$ MO that properly correlates the $2b_2$ orbital will probably look very different from the $8a_1$ MO necessary to correlate the $7a_1$ orbital. There are thus two "$8a_1$" MO's and we have here allowed the variational procedure to find and use the more important of the two.

The resulting state energies are displayed in Table 1 and drawn in Fig. 2. The fine details of these curves cannot, of course, be determined precisely from the widely separated values of interfragment separation (ΔR) appearing in Table 1. The curves of Fig. 2 are thus semi-schematic. Based on the arguments to be subsequently presented it is not believed that more precise curves for the least motion path would alter any conclusions presented here.

Table 1. Energies of various states of ketene as a function of C–C bond distance[a]

State	$^1A_1$	$^1A_1$[b]	$^3A_2$	$^1A_2$	$^3B_2$	$^1B_2$
$\Delta R = 0$	−151.6967 (−151.6721)[c]	−150.9368	−151.5574	−151.5500	−151.4676	−151.4615
$\Delta R = 2$	−151.5110	−151.4401	−151.3996	−151.3991	−151.5682	−151.4978
$\Delta R = 4$	−151.5544	−151.4297			−151.5926	−151.5200
$\Delta R = 10$	−151.5585	−151.4291			−151.5937	−151.5215

[a] Tabulated as R, the deviation of the C–C bond distance from the ketene equilibrium geometry value (in a. u.).

[b] Second lowest energy solution for the 6 configuration MC–SCF.

[c] Single configuration SCF energy.

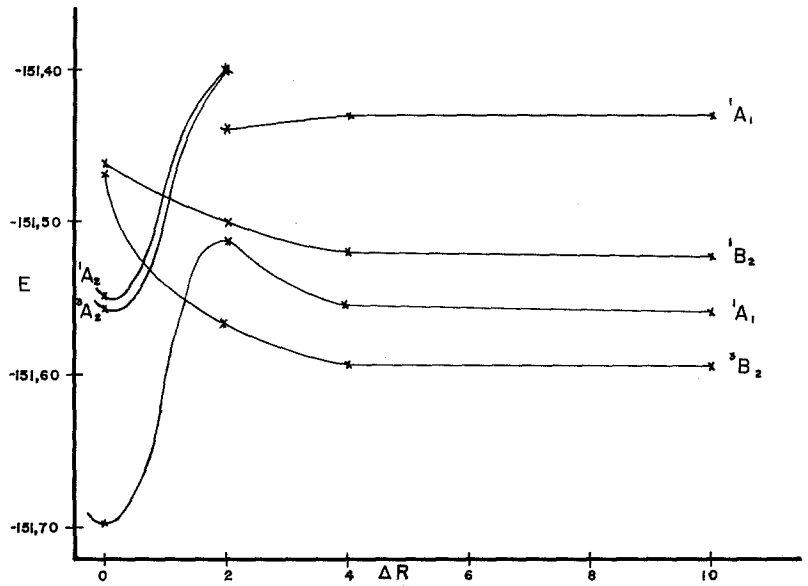

Fig. 2. Calculated state correlation diagram for the least motion path in $H_2CCO = CH_2 + CO$

Table 2. Orbital character of the valence molecular orbitals of ketene

$7a_1$	CO
$8a_1$	CH_2
$3b_1$	CO
$2b_2$	CH_2
$3b_2$	CO

The orbital character of the various relevant MO's as the interfragment separation becomes large is shown in Table 2. There are no differences among the multi or single configuration SCF results with regard to the orbital character of these MO's. The $2b_2 \rightarrow 3b_1(^{3,1}A_2)$ upper states are here seen to have the character of charge transfer states, $CH_2 \rightarrow CO$. However, probably at intermediate interfragment separations a $CO \rightarrow CO$ transition of this symmetry will drop lower in energy than the "charge transfer" state. This further justifies not taking the $^{1,3}A_2$ state calculations beyond $\Delta R = 2$ a.u. in the single configuration SCF formalism.

The $2b_2 \rightarrow 8a_1(^{3,1}B_2)$ states are here calculated to have substantial Rydberg character at the equilibrium ketene geometry, becoming pure valence as R increases. The relevant Rydberg basis orbital is centered primarily on the methylene carbon with almost no contribution from the carbonyl carbon Rydberg basis orbital. Price and co-workers [26] have identified several members of a Rydberg series in the electronic spectrum of ketene leading to an (adiabatic) ionization energy of 9.60 eV. This value of the first ionization potential is confirmed by the photoelectron spectroscopy (PES) study of Baker and Turner [27]. The quantum defect of $\delta \sim 1.07$ assigned by Price *et al.* [26] can be used to calculate

an (adiabatic) energy of 5.95 eV for the $n=3$ member of the series from the Rydberg formula. This compares with the calculated (vertical) $^1A_1 \rightarrow {}^1B_2$ excitation energy of 6.40 eV from Table 1. The band system observed by McGlynn and co-workers [8] with an (adiabatic) energy of 5.82 eV has the form of a Rydberg series (several sharp bands of decreasing intensity) and is similar to the first band system in the PES [27] where an interval of $\sim 1020\,cm^{-1}$ has also been observed and identified as a C – C = O stretch mode. A strong similarity in the intensity and vibrational frequency distributions between a Rydberg band system and the corresponding ionization process in the PES has been noted [28]. A measurement of the optical absorption spectrum at 2150–1950Å in condensed phase would establish the upper state orbital nature of the absorption in this region [29]. Such a drastic change in orbital character as a function of internuclear separation is not unknown; Mulliken has recently discussed several such cases [30].

Del Bene [15] has calculated that a $^3A_1$ state should lie just above the $^{1,3}A_2$ states but presumably still below the $^{1,3}B_2$ states. The equilibrium geometry for the $^3A_1$ state is calculated to be out-of-plane bent with an elongated C – C bond (1.54Å) relative to that in normal ketene (~ 1.32Å). This state arises essentially out of a $2b_2 \rightarrow 3b_2$ one electron transition and from Table 2 is thus seen to correlate with a $CO^3(\pi \rightarrow \pi^*)$ transition which begin at 6 eV in normal CO. This state can therefore not play on important role in the long wavelength photochemistry of ketene.

Discussion

The photodissociation reaction can now be discussed based on Fig. 2 and considerations previously outlined. The objective is to consider the feasibility of a near least motion path for the long wavelength photodissociation reaction. Again it should be emphasized that the curves in Fig. 2 are not precise even for the least-motion path and that, in any event, they will certainly be modified for their respective least energy paths. In the photolysis experiment at long wavelength ketene is apparently excited exclusively into the $^1A_2$ state which lies very close to and is interspersed with the vibronic levels of the $^3A_2$ state. There are several reasons for adopting this point of view. Firstly, no sensitized biacetyl emmission is observed using light between 2800 and 3660Å [31]. Then there is the cogent analysis of Laufer and Keller [9]. It is also quite reasonable to assume that where a singlet and triplet state are so close-lying the greater probability consistently resides in the singlet being preferentially populated for a given wavelength energy excitation in the range in which the 2 states overlap.

As a function of interfragment separation the rising $^{3,1}A_2$ curves are seen to cross the rapidly descending $^3B_2$ state, as expected. Geometry and configuration optimization would presumably moderate the climb rate of the A_2 states such that, all factors considered, the crossing in the least energy path would take place at lower relative energy for the $^1A_2$ state than shown while the avoided crossing of $^3A_2$ with $^3B_2$ (in the C_s geometry of an in-plane bent structure) will put the lower branch state at even lower energy. Formation of $^3CH_2$ from the $^3A_2$ state of ketene is thus seen to be favorable in a near least motion path with perhaps a small barrier to photodissociation. A more detailed analysis must

await a greater knowledge of the potential surface for the following reasons. The lowest energy $^3A_2$ vibronic levels presumably correspond to the in-plane bent equiblibrum geometry for this state. For these vibronic levels the barrier to photodissociation would be expected to be highest except that the more distorted the system is away from C_{2v} symmetry presumably the greater the interaction between $^3A_2$ and $^3B_2$ and hence (relatively speaking) the greater the tendency to the lower the barrier through configuration interaction.

The behavior of the $^1A_2$ and $^3B_2$ curves follows the same qualitative considerations for a near-least motion least energy path as for the $^3A_2$, $^3B_2$ pair with the additional need for intersystem crossing. Since an intersystem crossing is necessary for any mechanism that produces $^3B_2$ methylene from $^1A_2$ ketene its need cannot prejudice any given mechanism. With this in mind the near-least motion path looks reasonably favorable as the means of producing $^3CH_2$ from $^1A_2$ ketene. Of course, in long wavelength photolysis producing initially $^1A_2$ ketene there will be a higher barrier to overcome than starting with $^3A_2$ ketene.

The crossing of the $^1A_1$ and $^3B_2$ curves at intermediate interfragment separations means that initial excitation to the A_2 state of ketene could also be followed by the production of $^1CH_2$ depending on spin-orbit coupling strength, height of the barrier along the $^1A_1$ path, and $^1A_1 - {}^3B_2$ energy gap in CH_2 itself. This process could take place even at long wavelengths if the smoothing out of the barrier in the energy optimized path for the $^1A_1$ state allows the $^3B_2$ state to cross $^1A_1$ at lower energies than shown in Fig. 2. This is not definite, however, since the optimized geometry for $^3B_2$ is in-plane bent whereas the lowest energy path for $^1A_1$ is expected to be out-of-plane bent. Again it is a question of competing factors and there could be a number of no symmetry geometric conformers with similar probabilities for $^3B_2 \rightarrow {}^1A_1$ cross over.

The production of $^1A_1$ methylene ($^1CH_2$) from $^1A_2$ ketene at energies above the $^1A_1$ barrier does not at all appear feasible by a near-least motion departure, according to Fig. 2, even taking into account geometric relaxation. As pointed out [4] the close overlap and hence coupling between vibronic levels of $^1A_2$ and $^3A_2$ states should make the intersystem crossing rate between them particularly high. However, since precursor $^3A_2$ ketene is not observed as shown, for example, by the absence of an O_2 perturbation effect on the ketene spectrum [9] this mechanism cannot contribute significantly to the production of $^3CH_2$ and certainly not $^1CH_2$. The problem with the direct production of ground state $^1A_1$ methylene from $^1A_2$ ketene in a least motion path is that the $^1A_2$ and $^1A_1$ curves don't approach each other and hence their vibronic levels cannot couple which is required in order to obtain a transition rate between them. Of course, an in-plane bent near least motion path will lower the $^1A_2$ energy curves while possibly raising the $^1A_1$ energy which is expected to be out-of-plane bent in it's least energy path. Nonetheless, the gap in Table 1 and Fig. 2 appears rather too large to be bridged by any simple distortion of the least-motion path. The geometry optimized curves of Del Bene (Fig. 4) [15], when corrected for the proper behavior of the $^1A_1$ state, constitute important evidence in this regard.

Neither can the $^1B_2$ state play an important intermediary role here. The $^1A_1 \rightarrow {}^1B_2$ transition is electric dipole allowed in ketene and should be observed.

Although SCF calculations on singlet states can be difficult to interpret [20, 21] triplet states do not seem to present any such problem. Here the (vertical) $^3B_2$ state is calculated to fall at 5.58 eV above the single configuration SCF $^1A_1$ state (Table 1). It is difficult to imagine a spectroscopic triplet state lying below the calculated SCF state in the basis set used here. This fixes the corresponding spectroscopic $^1B_2$ state in the neighborhood of 6 eV in ketene. In methylene the $^1B_2 - {}^1A_1$ adiabatic energy difference is known experimentally [11] to be 0.88 eV. Although the geometry dependence of the $^1B_2$ state is not known it's very different orbital character from the $^1A_2$ state suggests that interaction between them will be small in geometric conformers in which such interaction is symmetry allowed. The $^1B_2$ curve is thus expected to always be above $^1A_1$.

For wavelengths around and below the dissociation energy to form $^1CH_2$ it is necessary to explore to what extent the lower vibronic levels of $^1A_2$ overlap and couple with the upper orbitational levels of the ground $^1A_1$ state in ketene. Absorption to $^1A_2$ begins at 2.65 eV [19] whereas $\Delta H^0_{f298^\circ}$ for $H_2CCO(^1A_1) = CH_2(^3B_2) + CO(^1\Sigma^+)$ is put at ~ 3.52 eV with the formation of $CH_2(^1A_1)$ at least 0.1 eV higher in energy [1]. Even according to Dixon and Kirby [7] who place the lowest absorption to the $^1A_2$ state at 3.22 eV such overlap exists [4]. The number of overlapping levels clearly depends on the height of the barrier to formation of $^1A_1$ but not necessarily along its least energy path where the barrier height is expected to be smallest. It would appear that the barrier is necessary in order to effect the stronger bound state-bound state coupling as opposed to bound-continium coupling which is not efficient for photodissociation processes in the absence of a curve crossing [32]. Clearly we must have more information about the multidimensional potential surface for these states in the neighborhood of the equilibrium geometry. Generally, however, it appears that for a near-least motion path at long wavelengths ($\lambda > 3300$ Å) the possibility at least exists for $^1A_2$ coupling with quasi-bound vibrational levels of the ground $^1A_1$ state above the dissociation energy to $^1CH_2$ with tunneling to the dissociated singlet products.

The photolytically generated $^1A_2$ state of ketene at long wavelength is thus seen to have two available channels in a near least motion path. To form $^3CH_2$ involves a spin-orbit coupling induced intersystem crossing to the $^3B_2$ state in the neighborhood of the intersection point of the two curves. Below the crossing point the probability to form $^3CH_2$ presumably decreases. The formation of $^1CH_2$ appears to be feasible only in the direction that a barrier to the thermal decomposition of ketene (to singlet products) exists. Under these circumstances it can be expected that the $^1A_2$ state will in general be relatively long-lived due to the absence of a rapid near-least motion relaxation path.

Rowland and co-workers [5, 6] have recently suggested that the ketene photodissociation reaction to form $^1CH_2$ goes through a 3 membered ring oxirene intermediate. The theoretical evidence presented here suggests that $^1CH_2$ will not be readily obtained in a near-least motion path. Since the ketene $^1A_2$ state is expected to be relatively longlived rearrangement of normal ketene to a ring structure before dissociation is a possibility. The question of the least energy path for the rearrangement process remains to be answered.

Acknowledgements. This work was supported by the U. S. National Bureau of Standards under grant number 1-35962.

References

1. Carr, R. W., Eder, T. W., Topor, M. G.: J. chem. Physics **53**, 4716 (1970).
2. Ho, S. Y., Noyes, W. A.: J. Amer. chem. Soc. **89**, 5091 (1967).
3. Strachan, A. N., Thornton, D. E.: Canad. J. Chem. **46**, 2353 (1968).
4. DeGraff, B. A., Kistiakowsky, G. B.: J. physic. Chem. **71**, 3984 (1967).
5. Montague, D. C., Rowland, F. S.: J. Amer. chem. Soc. **93**, 5381 (1971).
6. Russell, R. L., Rowland, F. S.: J. Amer. chem. Soc. **92**, 7508 (1970).
7. Dixon, R. N., Kirby, G. H.: Trans. Faraday Soc. **62**, 1406 (1966).
8. Rabalais, J. W., McDonald, J. M., Scherr, V., McGlynn, S. P.: Chem. Reviews **71**, 73 (1971).
9. Laufer, A. H., Keller, R. A.: J. Amer. chem. Soc. **93**, 61 (1971).
10. Chu, S. Y., Sui, A. K. Q., Hayes, E. F.: J. Amer. chem. Soc. **94**, 2969 (1972).
11. Hertzberg, G.: Electronic spectra of Polyatomic molecules. Princeton: Van Nostrand 1967.
12. O'Neal, S. V., Schaefer III, H. F., Bender, C. F.: J. chem. Physics **55**, 163 (1971); Del Bene, J. E.: Chem. Physics Letters **9**, 68 (1971).
13. Hoffmann, R., Woodward, R. B.: Accounts Chem. Res. **1**, 17 (1968).
14. Dobson, R. C., Hayes, D. M., Hoffmann, R.: J. Amer. chem. Soc. **93**, 6188 (1971); Hoffmann, R.: J. Amer. chem. Soc. **90**, 1475 (1968); Hoffmann, R., Gleiter, R., Mallory, F. B.: J. Amer. chem. Soc. **92**, 1460 (1970).
15. Del Bene, J.: J. Amer. chem. Soc. **94**, 3713 (1972).
16. Nesbet, R. K.: J. chem. Physics **43**, 4403 (1965).
17. Dunning, T. H.: J. chem. Physics **53**, 2823 (1970).
18. Huzinaga, S.: J. chem. Physics **42**, 1293 (1965).
19. Basch, H., McKoy, V.: J. chem. Physics **53**, 1628 (1970).
20. Basch, H.: Molecular Physics **23**, 683 (1972).
21. Basch, H., Robin, M. B., Kuebler, N. A.: J. chem. Physics **47**, 1201 (1967).
22. Dunning, T. H., Hunt, W. J., Goddard III, W. A.: Chem. Physics Letters **4**, 146 (1969).
23. Segal, G.: J. chem. Physics **53**, 360 (1970).
24. Basch, H.: J. chem. Physics **55**, 1700 (1971).
25. Das, G., Wahl, A. C.: J. chem. Physics **44**, 87 (1966).
26. Price, W. C., Teegan, J. P., Walsh, A. D.: J. chem. Soc. **1951**, 920.
27. Baker, C., Turner, D. W.: Chem. Comm. **1969**, 481.
28. Basch, H., Robin, M. B., Kiebler, N. A., Baker, C., Turner, D. W.: J. chem. Physics **51**, 52 (1969).
29. Robin, M. B., Kuebler, N. A.: J. molecular Spectroscopy **33**, 274 (1970); Miron, E., Raz, B., Jortner, J.: J. chem. Physics **56**, 5265 (1972).
30. Mulliken, R. S.: Chem. Physics Letters **14**, 137, 141 (1972).
31. Grossman, M., Semelick, G. P., Unger, I.: Canad. J. Chem. **47**, 3079 (1969).
32. Gebelein, H., Jortner, J.: Theoret. chim. Acta (Berl.) **25**, 143 (1972).

Prof. Harold Basch
Department of Chemistry
Bar Ilan University
Ramat Can
Israel